Journal of Alloys and Compounds 792 (2019) 46–49

Contents lists available at ScienceDirect

Journal of Alloys and Compounds

journal homepage: http://www.elsevier.com/locate/jalcom

A low ε_r and temperature-stable $Li_3Mg_2SbO_6$ microwave dielectric ceramics

Cuijin Pei [a, **], Caidan Hou [a], Yang Li [a], Guoguang Yao [a, b, *], Zhaoyu Ren [b], Peng Liu [c], Huaiwu Zhang [d]

[a] School of Science, Xi'an University of Posts and Telecommunications, Xi'an, 710121, China
[b] Institute of Photonics & Photon-Technology, Northwest University, Xi'an, 710069, China
[c] College of Physics and Information Technology, Shaanxi Normal University, Xi'an, 710062, China
[d] State Key Laboratory of Electronic Thin Films and Integrated Devices, University of Electronic Science and Technology of China, Chengdu, 610054, China

ARTICLE INFO

Article history:
Received 18 January 2019
Received in revised form
22 March 2019
Accepted 2 April 2019
Available online 3 April 2019

Keywords:
$Li_3Mg_2SbO_6$
Microwave dielectric properties
Sintering
Ceramics

ABSTRACT

$Li_3Mg_2SbO_6$ ceramics without dehiscence were prepared using a two-stage process. The sintering behavior, structure, and microwave dielectric performances of $Li_3Mg_2SbO_6$ ceramics had been investigated. XRD and Raman results showed that nearly pure phase $Li_3Mg_2SbO_6$ were obtained in the sintering temperature range of 1225–1350 °C. The quality factor (Qxf) and relative permittivity (ε_r) values of samples were strongly influenced by the density, grain size, and cell volume. Typically, balanced microwave dielectric properties were obtained for $Li_3Mg_2SbO_6$ ceramics sintered at 1300 °C:ε_r~10.5, Qxf~84,600 GHz (at 10.6 GHz), and temperature coefficient of resonance frequency τ_f ~ -9.0 ppm/°C.

1. Introduction

With rapid revolution of microwave components used in modern communication systems, new materials with high dielectric performance have drawn enormous attention for a wide range of microwave component applications, such as antennas and microwave substrates [1].

Microwave dielectric materials that can be used in the modern communication systems should have three key parameters: a low relative permittivity (ε_r) for reducing signal delay, a high quality factor (Qxf) for enhanced frequency selectivity and a near zero temperature coefficient of resonant frequency (τ_f) for temperature stability [2]. However, achieving all three parameters in one material is a formidable problem, because most of the low ε_r-microwave dielectric ceramics usually have high Qxf but highly negative τ_f values [3].

Recently, the orthorhombic structure of $Li_3Mg_2NbO_6$ ceramics with excellent microwave dielectric properties ($\varepsilon_r = 16.8$, Qxf = 79,643 GHz, $\tau_f = -27$ ppm/°C) was first reported by Bian et al. [4]. Later, Wu et al. [5] introduced its low loss characterization based on chemical bond theory. Many studies have been conducted to lower its sintering temperature, improve the microwave dielectric properties of $Li_3Mg_2NbO_6$-based ceramics by adding sintering aides, and partial Mg^{2+} ion substitution [6–10]. West et al. [11] reported that the $Li_3Mg_2SbO_6$ compound has the same structure as that of $Li_3Mg_2SbO_6$. However, few researches on the microwave dielectric properties of $Li_3Mg_2SbO_6$ ceramics have been reported, which is due to its dehiscence by reacting with individual oxide components [12]. Recently, Zhang et al. [13] reported that partial Sb^{5+} substitution for Nb^{5+} ions could gradually adjust its τ_f value near zero in $Li_3Mg_2(Nb_{1-x}Sb_x)O_6$ ($0.02 \le x \le 0.08$) materials systems. The similar phenomenon were also observed in other materials systems [14,15]. Thus, a novel $Li_3Mg_2SbO_6$ ceramics with balanced microwave dielectric properties (low ε_r, near zero τ_f, high Q) may be obtained. In our previous report, the secondary phase SbO_x in $Li_3Mg_2SbO_6$ ceramics deteriorates its Qxf value [12]. The low Qxf value and dehiscence of $Li_3Mg_2SbO_6$ ceramics limit its practical application in microwave devices. In this paper, pure phase $Li_3Mg_2SbO_6$ ceramics without dehiscence were synthesized using a two-stage process, and its sinterability, structure and microwave dielectric properties were also studied in detail.

* Corresponding author. School of Science, Xi'an University of Posts and Telecommunications, Xi'an, 710121, China.
** Corresponding author.
E-mail address: yaoguoguang@xupt.edu.cn (G. Yao).

https://doi.org/10.1016/j.jallcom.2019.04.019
0925-8388/

2. Experimental procedure

The $Li_3Mg_2SbO_6$ ceramics were prepared by a two-stage process using high-purity reagent of MgO, Sb_2O_3, and Li_2CO_3. First predried raw materials were weighed according to stoichiometric Li_3SbO_4, and ball-milled for 8 h with ethanol and agate balls as media. The obtained slurries were dried and then calcined at 900 °C for 4 h to form Li_3SbO_4 precursors. Second MgO and Li_3SbO_4 precursors were mixed in molar ratios of 2:1 and then ball-milled for 8 h. The dried powders were mixed with 5 wt% PVA, and pressed into cylindrical pellets with 10 mm in diameter and 5 mm in height under a pressure of 200 MPa. The green pellets were sintered at 1225 °C-1350 °C for 5 h in air.

The bulk densities of the sintered ceramics were measured using Archimedes' method. The crystalline phases were analyzed by X-ray powder diffraction (XRD) with CuKα radiation (RigakuD/MAX2550, Tokyo, Japan). The Raman spectra were collected at room temperature using a Raman Microscope (Horiba Jobin Yvon S.A.S., France) with He-Ne laser (633 nm) operated at 30 mW. The surface microstructure of pellets was characterized by scanning electron microscope (SEM, Fei Quanta 200, Eindhoven, Holland) and the grain size was estimated using the image analysis software (Image Tool for Windows version 3.00, Microsoft, Redmond, WA). The microwave dielectric properties of sintered samples were measured using a network analyzer (ZVB20, Rohde & Schwarz, Germany) with the $TE_{01\delta}$ shielded cavity method. The τ_f was calculated with the following equation (1):

$$\tau_f = \frac{f - f_0}{f_0 \times (T - T_0)} \times 10^6 \quad (1)$$

where f and f_0 are the resonant frequency at T (80 °C) and T_0 (20 °C), respectively.

3. Result and discussion

Fig. 1 illustrates the powder XRD patterns of $Li_3Mg_2SbO_6$ (LMS) ceramics fired at different temperatures. It can be found that all samples showed mixture phases with $Li_3Mg_2SbO_6$ main phase (orthorhombic: JCPDS No. 86-0345) along with small amount of unknown phase marked with stars. Furthermore, the enlargement of (111) main peak is shown in the inset of Fig. 1, with increasement of firing temperature, the reflection peak (111) initially shifted to lower angle and then to higher angle again. In order to further investigate the abnormal change in detail, the XRD data of the sintered specimens were refined based on Rietveld method through a GSAS software. We adopted $Li_3Co_2TaO_6$ (ICSD #81043) as the starting model, and the corresponding refinement results are given in Fig. 2 and Table 1. From the data in Table 1, the change of the lattice parameters is in agreement with the above discussion in illustration of Fig. 1. As it was reported that oxygen vacancy causes lattice expansion whereas the cation vacancy leads lattice contraction [16–18]. In our cases, the abnormal change in the main peak (111) could attributed to the competitive results of the volatilization of Li^+ ions and the formation of oxygen vacancies at high temperatures.

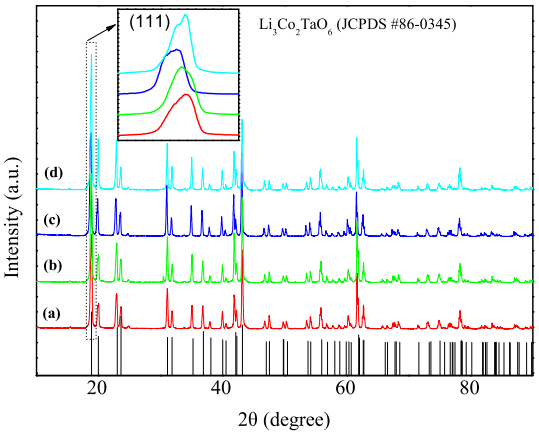

Fig. 1. XRD patterns of LMS ceramics sintered at different temperatures:(a)1250 °C, (b) 1275 °C, (c)1300 °C, (b)1325 °C.

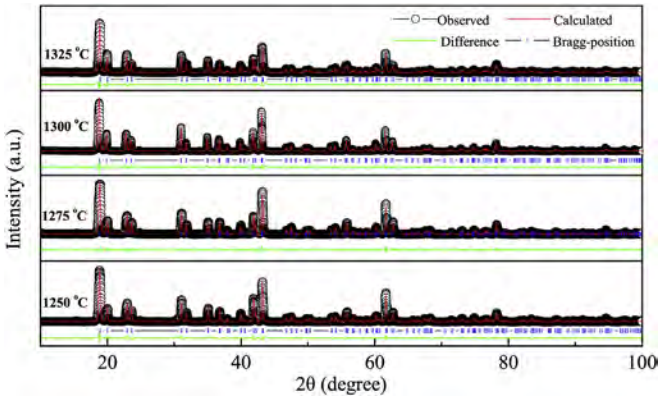

Fig. 2. Rietveld refinement patterns of LMS ceramics sintered at various temperatures.

The typical Raman spectroscopy for LMS ceramics with various sintering temperatures are shown in Fig. 3. Three phonon modes were observed and located around 473, 552, and 657 cm^{-1}, which agreed reasonably well with the signature of $Li_3Mg_2NbO_6$-based ceramics [8]. The strong peak at 657 cm^{-1} is related to the stretching vibration of Sb—O, while the other peaks are assigned to the Li/Mg—O bonds vibration [8,19].

Fig. 4 displays the typical surface SEM images of LMS ceramics sintered at various temperatures. As shown in Fig. 4(a)-(c), all the samples exhibited porous microstructure, and the apparent porosity decreased and the average grain size increased as the sintering temperature rising. A compact microstructure with an average grain size about 15.3 μm could be obtained for the specimen fired at 1300 °C. However, when the sintering temperature surpassed 1300 °C, enlarged grain growth and micro-crack occurred as shown in Fig. 4(e) and (f), which would degrade its

Table 1
Refinement parameters and reliability factors of $Li_3Mg_2SbO_6$ ceramics with different sintering temperatures.

T (°C)	a (Å)	b (Å)	c (Å)	cell volume (Å^3)	packing fraction (%)	R_p	R_{wp}
1250	5.9404	8.5175	17.7371	897.4503	69.99	10.20	14.51
1275	5.9426	8.5934	17.7161	904.7100	69.43	10.21	13.91
1300	5.9302	8.6436	17.8319	914.0430	68.72	8.96	12.50
1325	5.9053	8.6000	17.8440	906.2178	69.31	10.08	14.74

T: sintering temperature; R_{wp}: the reliability factor of weighted patterns; R_p: the reliability factor of patterns.

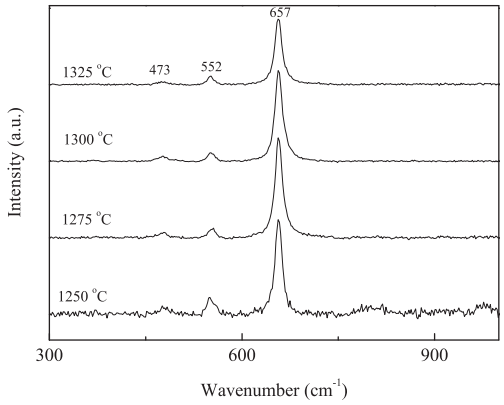

Fig. 3. Typical Raman spectroscopy for LMS ceramics fired at different temperatures.

density and dielectric properties.

Fig. 5 illustrates the relative density and microwave dielectric properties of LMS ceramics at different sintering temperatures. As illustrated in Fig. 5(a), the relative density of specimens initially increased and reached the maximum value at 1300 °C, then declined with a rise in sintering temperature. This result coincides well with the SEM observation where the abnormal grain growth and micro-crack result in low relative density. As the sintering temperature increased from 1225 to 1350 °C, the ε_r also rose and declined thereafter. The maximum ε_r value was obtained at 1325 °C and not at the optimum densification temperature 1300 °C. The ε_r is determined by density, dielectric polarizability, molecular volume, and the ε_r decreases as molecular volume increases [20]. In our cases, the improvement in ε_r value with a rise in sintering temperature was attributed to the enhancement in relative density and the decrease in molar volume (seen in Table 1). It is well known that the Qxf value is affected by both intrinsic factors relying on the crystal structure and packing fraction and extrinsic factors

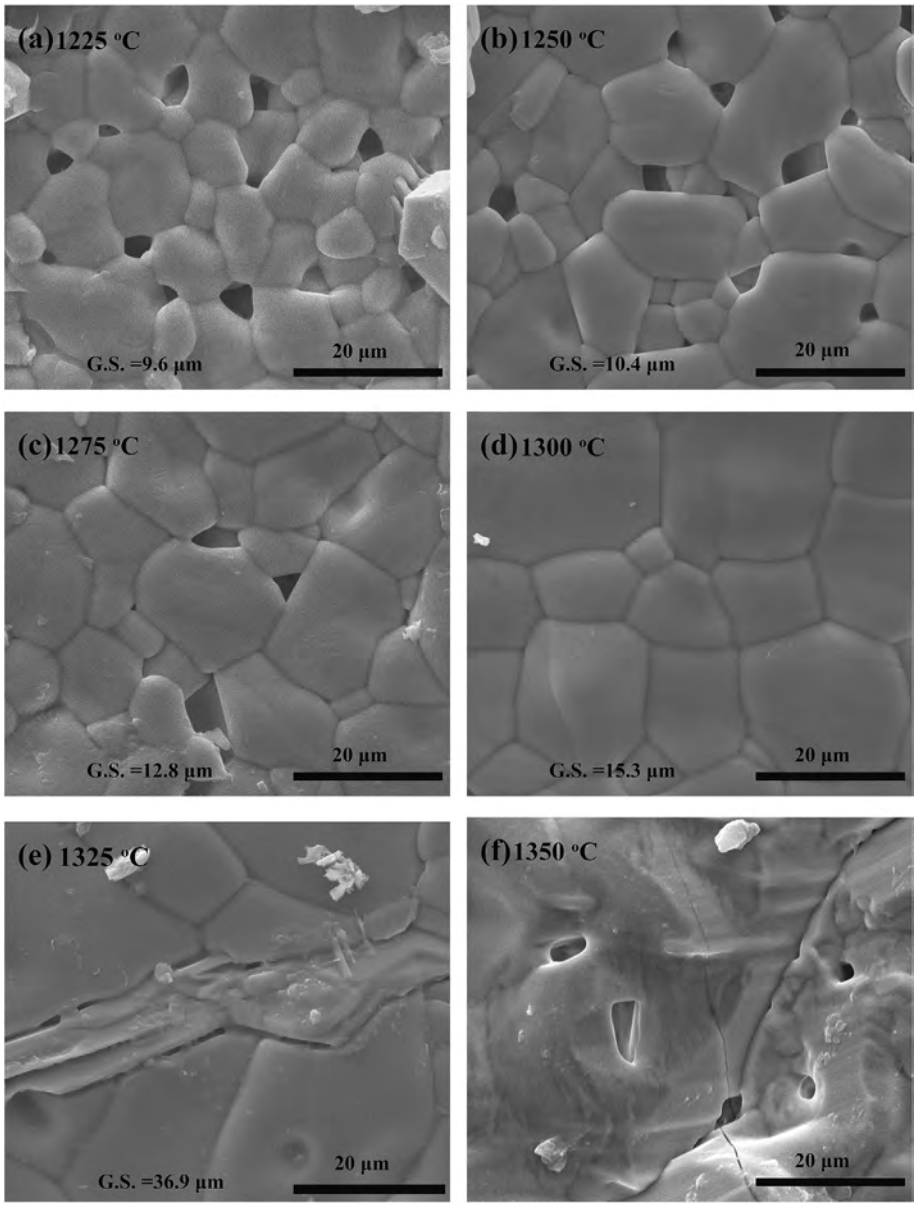

Fig. 4. Typical surface SEM images of LMS ceramics sintered at various temperatures.

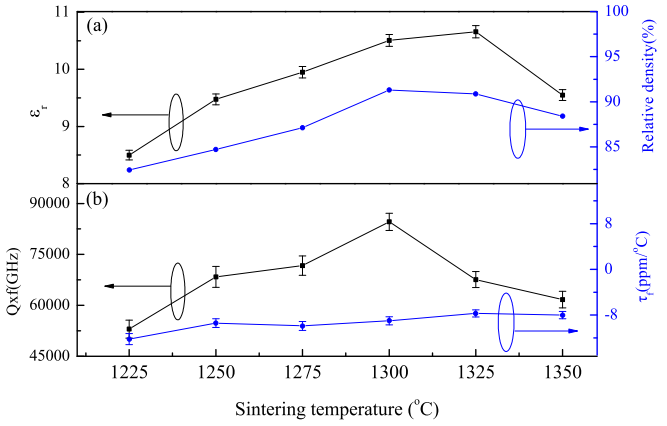

Fig. 5. Variations of relative density and microwave dielectric properties of LMS ceramics as a function of sintering temperature.

determined by average grain size, relative density, secondary phase, defects, etc [21,22]. As shown in Fig. 5(b), the trend between the Qxf and sintering temperature exhibited an identical tendency as that of relative density vs sintering temperature, implying that the Qxf value was mainly influenced by the extrinsic dielectric loss rather than intrinsic loss. The improvement in Qxf value with increasing firing temperature is ascribed to the increase in the relative density as well as average grain size [23]. And the deterioration in Qxf value at higher temperatures could attribute to the poor microstructure [24]. The τ_f values of the samples were insensitive to the sintering temperature and fluctuated around −9.0 ppm/°C, because no alternate composition was observed at different temperatures.

4. Conclusion

$Li_3Mg_2SbO_6$ ceramics without dehiscence were synthesized via a two-stage process and its sintering behavior, structure, and microwave dielectric performances were investigated. The XRD and Raman results showed that nearly pure phase $Li_3Mg_2SbO_6$ ceramics with an orthorhombic structure were obtained in sintering temperature range of 1225–1350 °C. The ε_r values of samples were highly dependent on the porosity and cell volume, while their Qxf values were mainly relative to the microstructure. In particular, the $Li_3Mg_2SbO_6$ ceramics sintered at 1300 °C exhibited balanced microwave dielectric properties with $\varepsilon_r = 10.5$, Qxf = 84,600 GHz (at 10.6 GHz) and τ_f = -9 ppm/°C. Further work is in progress to lower its sintering temperature and ameliorate its dielectric performances to meet the LTCC application requirements.

Acknowledgements

This work is supported by the National Natural Science Foundation of China (Grant No 51402235). China's Post-doctoral Science Fund (Grant No. 2015M582696), and by Shaanxi Province Postdoctoral Science Foundation. Shaanxi Province Department Education (No. 18JK0711).

References

[1] C.C. Li, C.Z. Yin, J.Q. Chen, H.C. Xiang, Y. Tang, L. Fang, Crystal structure and dielectric properties of germanate melilites $Ba_{[2]}MGe_{[2]}O_{[7]}$ (M = Mg and Zn) with low permittivity, J. Eur. Ceram. Soc. 38 (2018) 5246–5251.
[2] R.Z. Zuo, Y.D. Xu, M. Shi, W.Q. Li, L.G. He, A new series of low-temperature cofirable $Li_3Ba_2La_{3(1-x)}Y_{3x}(MoO_4)_8$ microwave dielectric ceramics, J. Eur. Ceram. Soc. 38 (2018) 4677–4681.
[3] C.L. Huang, Y.W. Tseng, Structure, dielectric properties, and applications of $CaTiO_3$-modified $Ca_4MgNb_2TiO_{12}$ ceramics at microwave frequency, J. Am. Ceram. Soc. 94 (2011) 1824–1828.
[4] L.L. Yuan, J.J. Bian, Microwave dielectric properties of the lithium containing compounds with rock salt structure, Ferroelectrics 387 (2009) 123–129.
[5] H.T. Wu, E.S. Kim, Characterization of low loss microwave dielectric materials $Li_3Mg_2NbO_6$ based on the chemical bond theory, J. Alloys Compd. 669 (2016) 134–140.
[6] T.W. Zhang, R.Z. Zuo, Effect of $Li_{[2]}O$-$V_{[2]}O_{[5]}$ addition on the sintering behavior and microwave dielectric properties of $Li_{[3]}(Mg_{1-x}Zn_x)_{[2]}NbO_{[6]}$ ceramics, Ceram. Int. 40 (2014) 15677–15684.
[7] P. Zhang, L. Liu, M. Xiao, Microwave dielectric properties of high Q and temperature stable $Li_{[3]}(Mg_{1-x}Ni_x)_{[2]}NbO_{[6]}$ ceramics, J. Mater. Sci. Mater. Electron. 29 (2018) 5057–5063.
[8] C.F. Xing, J.X. Bi, H.T. Wu, Effect of Co-substitution on microwave dielectric properties of $Li_3(Mg_{1-x}Co_x)_2NbO_6$ ($0.00 \leq x \leq 0.10$) ceramics, J. Alloy. Comp. 719 (2017) 58–62.
[9] P. Zhang, L. Liu, M. Xiao, Y.G. Zhao, A novel temperature stable and high Q microwave dielectric ceramic in $Li_3(Mg_{1-x}Mn_x)_2NbO_6$ system, J. Mater. Sci. Mater. Electron. 28 (2017) 12220–12225.
[10] T.W. Zhang, R.Z. Zuo, C. Zhang, Preparation and microwave dielectric properties of $Li_3(Mg_{0.92}Zn_{0.08})_2NbO_6$-$Ba_3(VO_4)_2$ composite ceramics for LTCC applications, Mater. Res. Bull. 68 (2015) 109–114.
[11] M. Castellanos, J.A. Gard, A.R. West, Crystal data for a new family of phases, $Li_3Mg_2XO_6$: X=Nb, Ta, Sb, J. Appl. Crystallogr. 15 (1982) 116–119.
[12] G.G. Yao, C.J. Pei, Z.Y. Ren, P. Liu, Microwave dielectric properties of temperature stable (1-x)$Li_3Mg_2SbO_6$-x$Ba_3(VO_4)_2$ composite ceramics, J. Mater. Sci. Mater. Electron. 29 (2018) 9979–9983.
[13] P. Zhang, S.X. Wu, M. Xiao, Effect of Sb^{5+} ion substitution for Nb^{5+} on crystal structure and microwave dielectric properties for $Li_3Mg_2NbO_6$ ceramics, J. Alloys Compd. 766 (2018) 498–505.
[14] N. Wang, M.Y. Zhao, W. Li, Z.W. Yin, The sintering behavior and microwave dielectric properties of Bi(Nb,Sb)O_4 ceramics, Ceram. Int. 30 (2004) 1017–1022.
[15] W.S. Xia, G.Y. Zhang, L.W. Shi, M.M. Zhang, Enhanced microwave dielectric properties of $ZnTa_{[2]}O_{[6]}$ ceramics with Sb^{5+} ion substitution, Mater. Lett. 124 (2014) 64–66.
[16] L.W. Tai, M.M. Nasrallah, H.U. Anderson, D.M. Sparlin, S.R. Sehlin, Structure and electrical properties of $La_{1-x}Sr_xCo_{1-y}Fe_yO_3$. Part 1. The system $La_{0.8}Sr_{0.2}Co_{1-y}Fe_yO_3$, Solid State Ionics 76 (1995) 259–271.
[17] Y. Dang, A.R. West, Oxygen stoichiometry, chemical expansion or contraction, and electrical properties of rutile, $TiO_{2\pm\delta}$ ceramics, J. Am. Ceram. Soc. 102 (2019) 251–259.
[18] G.G. Yao, P. Liu, X.G. Zhao, J.P. Zhou, H.W. Zhang, Low-temperature sintering and microwave dielectric properties of $Ca_5Co_4(VO_4)_6$ ceramics, J. Eur. Ceram. Soc. 34 (2014) 2983–2987.
[19] R.L. Frost, S. Bahfenne, A Raman spectroscopic study of the antimony mineral klebelsbergite $Sb_4O_4(OH)_2(SO_4)$, J. Raman Spectrosc. 42 (2011) 219–223.
[20] E.S. Kim, C.J. Jeon, P.G. Clem, Effects of crystal structure on the microwave dielectric properties of ABO_4 (A = Ni, Mg, Zn and B = Mo, W) ceramics, J. Am. Ceram. Soc. 95 (2012) 2934–2938.
[21] L.X. Pang, D. Zhou, Z.M. Qi, Z.X. Yue, I.M. Reaney, Structure-property relationships of low sintering temperature scheelite-structured (1- x)$BiVO_4$-x$LaNbO_4$ microwave dielectric ceramics, J. Mater. Chem. C. 5 (2017) 2695–2701.
[22] V.L. Gurevich, A.K. Tagantsev, Intrinsic dielectric loss in crystals, Adv. Phys. 40 (1991) 719–767.
[23] C.F. Teng, Microwave dielectric properties of a new ultra low loss pervoskite ceramic, J. Am. Ceram. Soc. 91 (2008) 4125–4128.
[24] M. Valant, D. Suvorov, Microstructural phenomena in low-firing ceramics, Mater. Chem. Phys. 79 (2003) 104–110.